Evidence of electron saddle swap oscillations in angular differential ion–atom charge exchange cross sections

2012 J. Phys. B: At. Mol. Opt. Phys. 45 175201

(http://iopscience.iop.org/0953-4075/45/17/175201)

J. Phys. B: At. Mol. Opt. Phys. **45** (2012) 175201 (6pp) doi:10.1088/0953-4075/45/17/175201

Evidence of electron saddle swap oscillations in angular differential ion–atom charge exchange cross sections

S Otranto[1], I Blank[2], R E Olson[3] and R Hoekstra[2]

[1] IFISUR and Departamento de Física, Universidad Nacional del Sur, 8000 Bahía Blanca, Argentina
[2] KVI Atomic Physics, Zernikelaan 25, NL-9747 AA, Groningen, The Netherlands
[3] Physics Department, Missouri University of Science and Technology, Rolla, MO 65409, USA

E-mail: sotranto@uns.edu.ar

Received 30 April 2012, in final form 9 July 2012
Published 9 August 2012
Online at stacks.iop.org/JPhysB/45/175201

Abstract
State selective charge exchange processes in 1–10 keV/amu Ne^{8+} +Na(3s) collisions were measured by means of the magneto-optical trap recoil-ion momentum spectroscopy technique and compared to classical trajectory Monte Carlo calculations. We find that for electron capture to n-levels $\geqslant 10$, the transverse momentum distributions exhibit an oscillatory structure which is very sensitive to the impact energy. Our theoretical analysis suggests that this feature is a direct consequence of the number of swaps the electron undergoes across the potential energy saddle during the charge exchange process.

(Some figures may appear in colour only in the online journal)

Introduction

The theoretical description of atom–atom and ion–atom collisions has been spurred by the experimental observation of an unexpected structure in both total and differential cross sections. Early on, regular oscillations in atom–atom total cross sections led groups such as that of Bernstein to interpret them as being due to a region of the stationary phase produced by the attractive well in the atom–atom potential [1]. Since quantal phase shifts vary as $1/v$ at high energies, indexing the maxima and minima and plotting them versus $1/v$ lead to new information about atom–atom potential well depths and equilibrium positions.

Similar $1/v$ oscillatory behaviour was reported for keV energy ion–atom collisions for both symmetric and inelastic alkali ion–alkali atom charge exchange systems [2]. Here, oscillations on the total cross sections were interpreted as being due to a region of the stationary phase in the difference between the incident and outgoing channels [3]. Stationary phases arise when there is a maximum in the difference potential between the incident and product channels or when these two potential energy states are parallel to one another inside the transition region. Again a quantal or semi-quantal description of collisions was necessary.

Very recently, oscillations in the total cross sections for ion–Rydberg atom charge exchange collisions were observed [4]. Interestingly, a classical description of their origin was invoked and used to explain the structure as being due to the active electron swapping centres during the collision, not in terms of a stationary phase argument, even though the oscillations were evenly spaced in $1/v$. The rational was that classical trajectory Monte Carlo (CTMC) calculations nicely reproduced the structure; there is no phase information in CTMC calculations. Note that for these Rydberg systems and for the one we present, the study of the scattering via more rigorous atomic- or molecular-orbital quantal methods represents a very difficult task due to the large density of the final states available.

Schultz *et al* elaborated on the electron swap thesis and showed that the oscillatory total cross section for He^{2+} + H excitation was also due to electron swaps [5]. In a follow-up paper, Krstic *et al* then gave a quantal description of this specific reaction and showed that the oscillations originate from the phase interference of two paths beginning from the initial state leading to a common final state [6].

In this paper we focus our studies on Ne^{8+} + Na(3s) collisions showing that these 'electron swaps' are quite general and exist on both total cross sections and on their

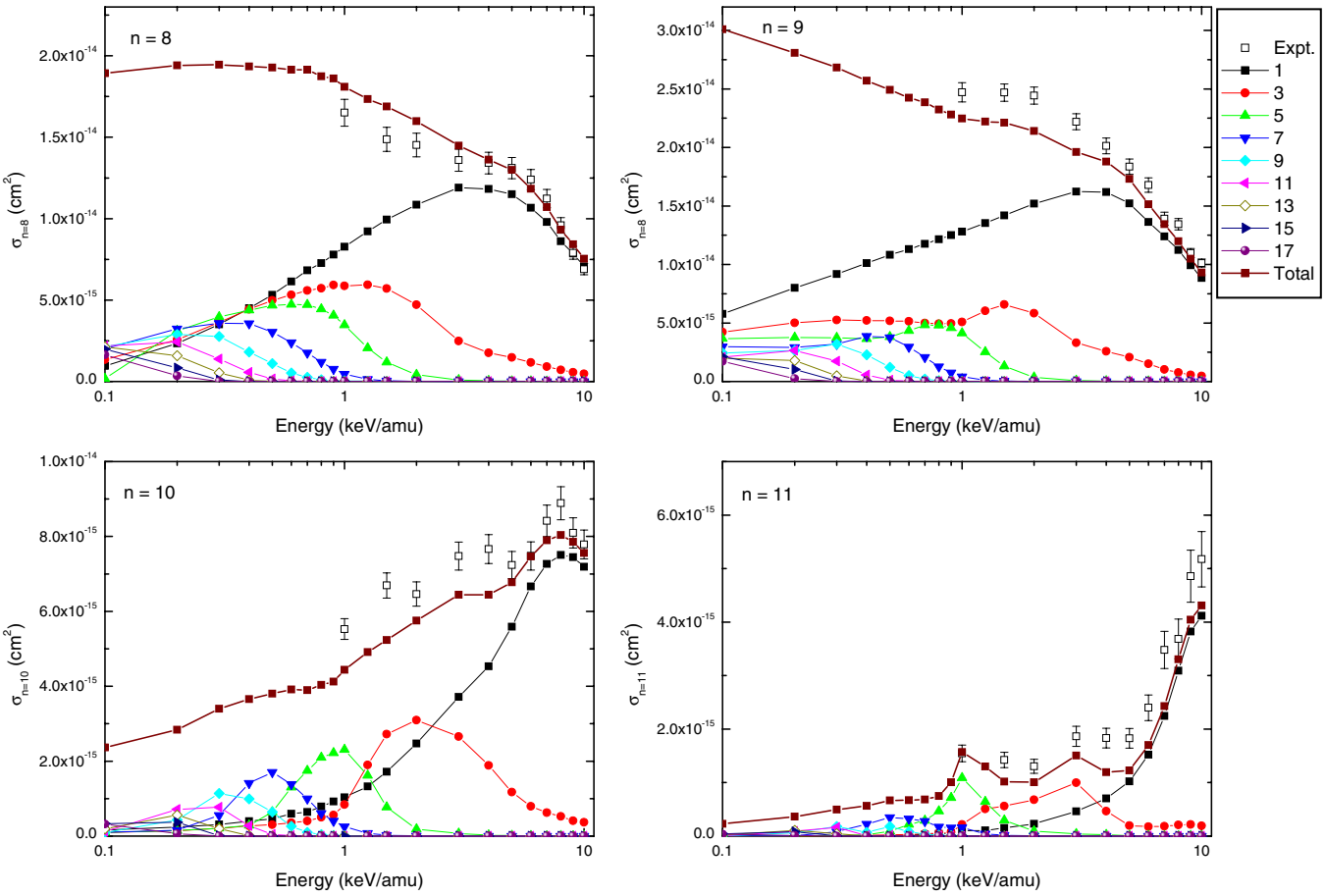

Figure 1. Capture cross sections to $n = 8$–11 for Ne^{8+}+Na(3s) collisions. The partial contributions arising from different numbers of swaps are explicitly shown. The experimental data are given by open squares.

corresponding angular differential ion–atom ones. We show that these swap oscillations persist to high-lying product states and are connected with the widely applied Coulomb-over-the-barrier model [7]. Moreover, even though the swap oscillations in the total cross sections decrease in magnitude as one goes to lower collision energies due to the integration of the increasing number of swaps over all impact parameters, the differential cross sections still show major signatures of each swap as a function of scattering angle. For such observations of highly charged projectiles, very high resolution data for scattering angles are necessary and can only be achieved via the use of a cold target in combination with recoil-ion momentum spectroscopy [8–10].

The experimental method

Measurements for the present collision system were carried out in the energy range 1–10 keV/amu by means of the magneto-optical trap (MOT) recoil-ion momentum spectroscopy device developed at KVI. Since our apparatus has been described elsewhere [11, 12] only a brief outline will be given here. Sodium atoms are cooled and trapped in a MOT using a magnetic field of 20 Gauss cm^{-1} and three counter-propagating laser beams with a diameter of 20 mm each. The total light intensity is of about 100 mW. Our ion beam is collimated to 1 mm and crossed with the MOT. The resulting Na^+ ions are extracted transverse to the ion beam direction by a low electric field (<0.5 V cm^{-1}) and their 2D position is recorded in our detector. The resolution is 0.05 au in the longitudinal direction and about 0.2 au for the transverse momentum spectra [13]. From the longitudinal component of the Na^+ recoil momentum, the Q-value of the collision can be deduced, and hence the product n-level.

The theoretical model

The obtained data are contrasted against CTMC calculations which rely on the numerical evaluation of a mutually interacting three-body system. For the Na^+ core interaction with the electron and the projectile, we have used the central model potential of Garvey *et al* [14] where the effective charge seen by the active electron and the projectile depend on their radial distances with respect to the target core. The usual Becker and McKellar binning condition [15] is applied to obtain the state selective capture cross sections.

In our CTMC code, an electron swap is recorded each time the electron position vector component along the internuclear axis ($r_e \cdot R$) crosses the potential saddle position $r_{\rm saddle}$, which is a function of the internuclear distance R. Once the electron's energy overcomes the potential barrier it can move in the field of both ions during a lapse directly determined by the impact energy and the impact parameter. In this sense, as the impact

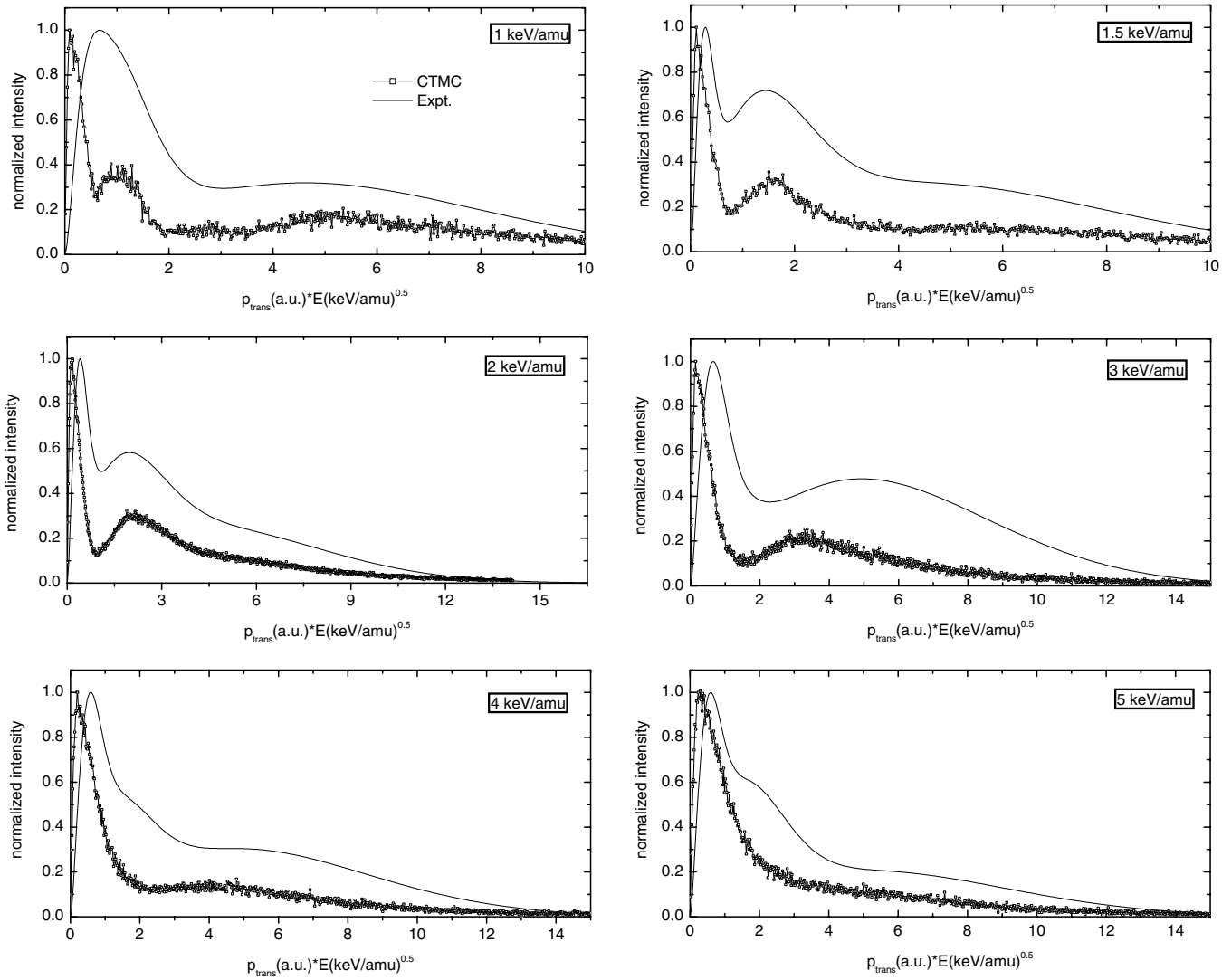

Figure 2. $p_{\rm trans}$ distributions for 1–5 keV/amu Ne^{8+}+Na(3s) collisions leading to capture to $n = 10$ as a function of $p_{\rm trans}$*E(keV/amu)$^{1/2}$. Solid line: experimental data; open squares: CTMC results. The results were normalized to unity at their peak positions.

energy is lowered, the time gap during which the electron can be pushed back and forth between centres increases, and as such, the total number of swaps. For the present Garvey representation of the target, the position of the saddle can be parametrized as $r_{\rm saddle} = r_{\rm COB} + aR^2\,{\rm e}^{-\lambda R} + bR^2\,{\rm e}^{-\gamma R}$, with $r_{\rm COB} = R/(\sqrt{Z_p}+1)$ (the saddle position predicted by the classical overbarrier model for the hydrogen target) and $a = 0.56$, $b = 0.12$, $\mathrm{l} = 1.37$ and $\mathrm{g} = 0.39$ the parameters corresponding to the correction terms. From the above parametrization, we can observe that compared to the hydrogenic model, the Garvey model shifts the potential saddle to larger distances for low R values. This clearly indicates that for the present case the target ion's area of influence extends to larger distances than predicted by the standard overbarrier prediction.

Results

In figure 1, we show the n-state selective total charge exchange cross sections (σ_n) for $n = 8$–11. The present results complement those shown in a recent article [12] by considering a wider energy range. CTMC calculations are shown down to an impact energy of 0.1 keV/amu, clearly highlighting the presence of distinctive structures for each n-value. The partial contribution of trajectories involving different numbers of swaps during the charge exchange process is explicitly shown. At the higher impact energies explored experimentally, our theoretical results are in very good agreement with the measured data clearly indicating that the structure in the obtained profiles for the different n-values corresponds to the superposition of contributions from 1- and 3-swap trajectories, which maximize at different impact energies. As the impact energy decreases, the possible number of contributing swaps increases as shown, building the low energy tails of the distributions. For the higher n-values considered, the different swaps preserve a more localized peaked contribution which leads to a stronger oscillatory behaviour.

A more stringent inspection of the role the different swaps play during the charge exchange process can be performed by exploring the momentum acquired by the recoiling target ion (p_R) after the charge exchange. Its longitudinal component ($p_{\rm l}$) is directly related to the final n-value to which the electron

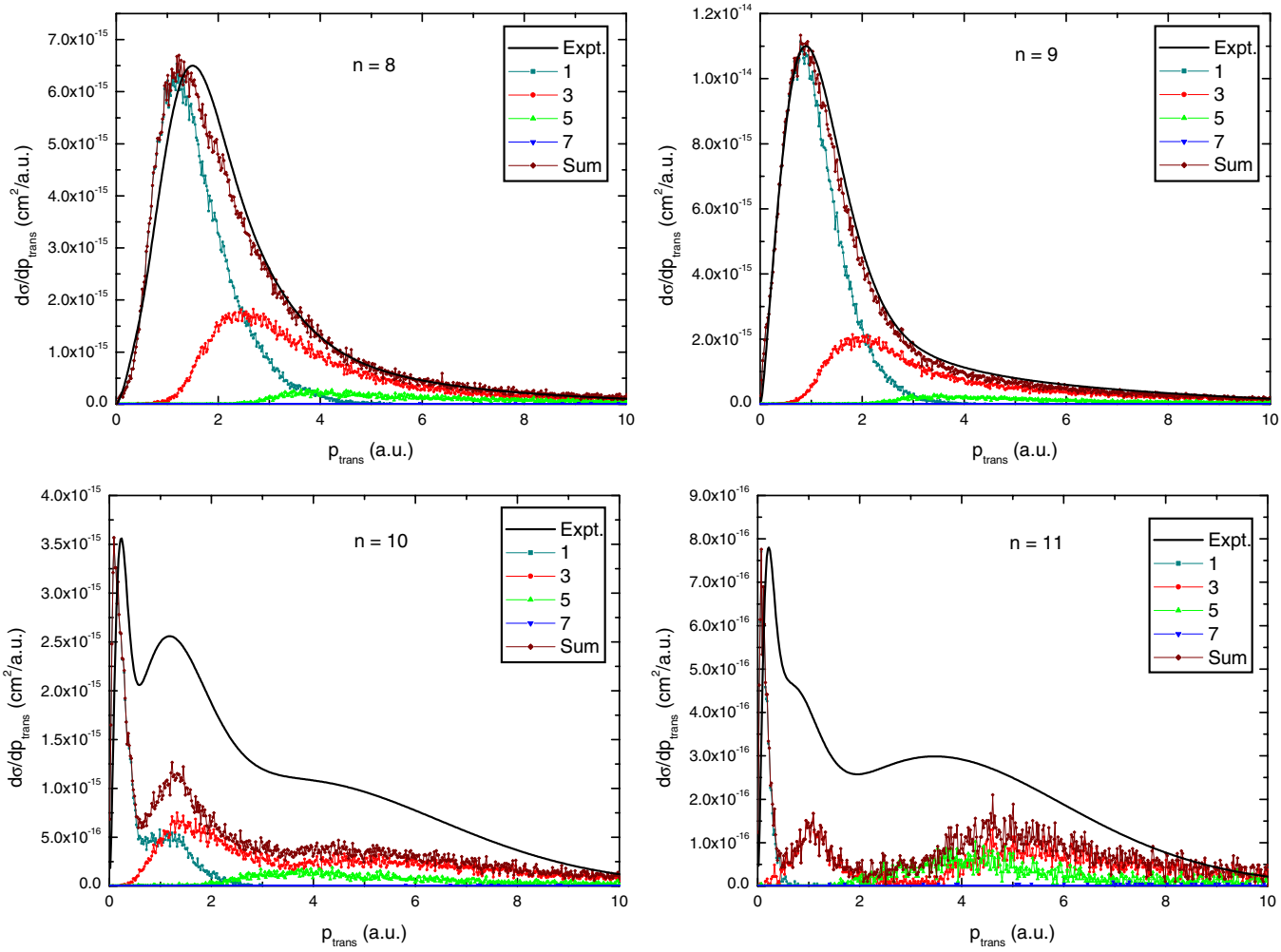

Figure 3. Experimental and theoretical $p_{\rm trans}$ distributions for 1.5 keV/amu Ne^{8+}+Na(3s) collisions leading to electron capture to $n = 8$–11. The CTMC partial contributions arising from different numbers of saddle crossings are explicitly shown. The experimental results were normalized to the CTMC peak values.

is captured, while the transverse component ($p_{\rm trans}$) provides detailed information on the trajectory of the scattered projectile since $p_{\rm trans} = m_P v\theta_{\rm scatt}$, where m_P is the projectile mass and v is the projectile velocity.

In figure 2, we show the scaled $p_{\rm trans}$ distributions for electron capture to $n = 10$. We note for the 2 keV/amu case a minimum at $p_{\rm trans}$ close to 0.66 au which washes out as the impact energy increases to 5 keV/amu. For impact energies larger than 5 keV/amu, traces of such structure cannot be inferred from our data. The present CTMC results, on the other hand, closely follow the profile of the distribution as well as the strong energy dependence exhibited by the data. Note that the experimental resolution was not adequate in order to discern the lowest $p_{\rm trans}$ peak shown in the calculations at 1 keV/amu.

In figure 3, we show the experimental and theoretical $p_{\rm trans}$ distributions for 1.5 keV/amu Ne^{8+}+Na(3s) collisions leading to electron capture to $n = 8$–11. The $p_{\rm trans}$ CTMC separate contributions from the different swap trajectories for each n-value are explicitly shown. For $n = 8$ and 9, we observe very good agreement between theory and experiment. For $n = 10$ and 11 the agreement worsens, but the main structures are correctly reproduced. These are due to the superposition of the 1-, 3- and 5-swap contributions which peak separately enough in $p_{\rm trans}$ so as to allow the different peaks to be observed. For $n \leqslant 9$, we have not observed such a structure at any impact energy explored with the CTMC. The contributions from 1-, 3- and 5-swaps in these cases add up, leading to a smooth $p_{\rm trans}$ distribution as inferred from figure 3. However, for larger n-values such as $n = 11$, we again observe a strong oscillatory behaviour in the energy range explored. It seems clear from the $n = 10$ and 11 cases shown that the oscillations are not only due to the summed contributions arising from different swaps, but 1- and 3-swap mechanisms can provide the structures by themselves. To trace back the origin of these structures, in figure 4 we present the corresponding event plots of $p_{\rm trans}$ as a function of the projectile's z-coordinate at which the last saddle crossing took place ($z_{\rm last\ crossing}$). For $n = 10$, we see that the peak at low $p_{\rm trans}$ values for the 1-swap mechanism mainly corresponds to collisions in which the last saddle crossing takes place once the projectile passes the reaction region ($+10$ au $< z_{\rm last\ crossing} < +30$ au). The structure seen at about 1.2 au, on the other hand, is formed in the incoming channel of the projectile (-15 au $< z_{\rm last\ crossing} < -5$ au). The 3-swap mechanism also shows a peak at $p_{\rm trans} \approx 1.5$ au and a second less prominent

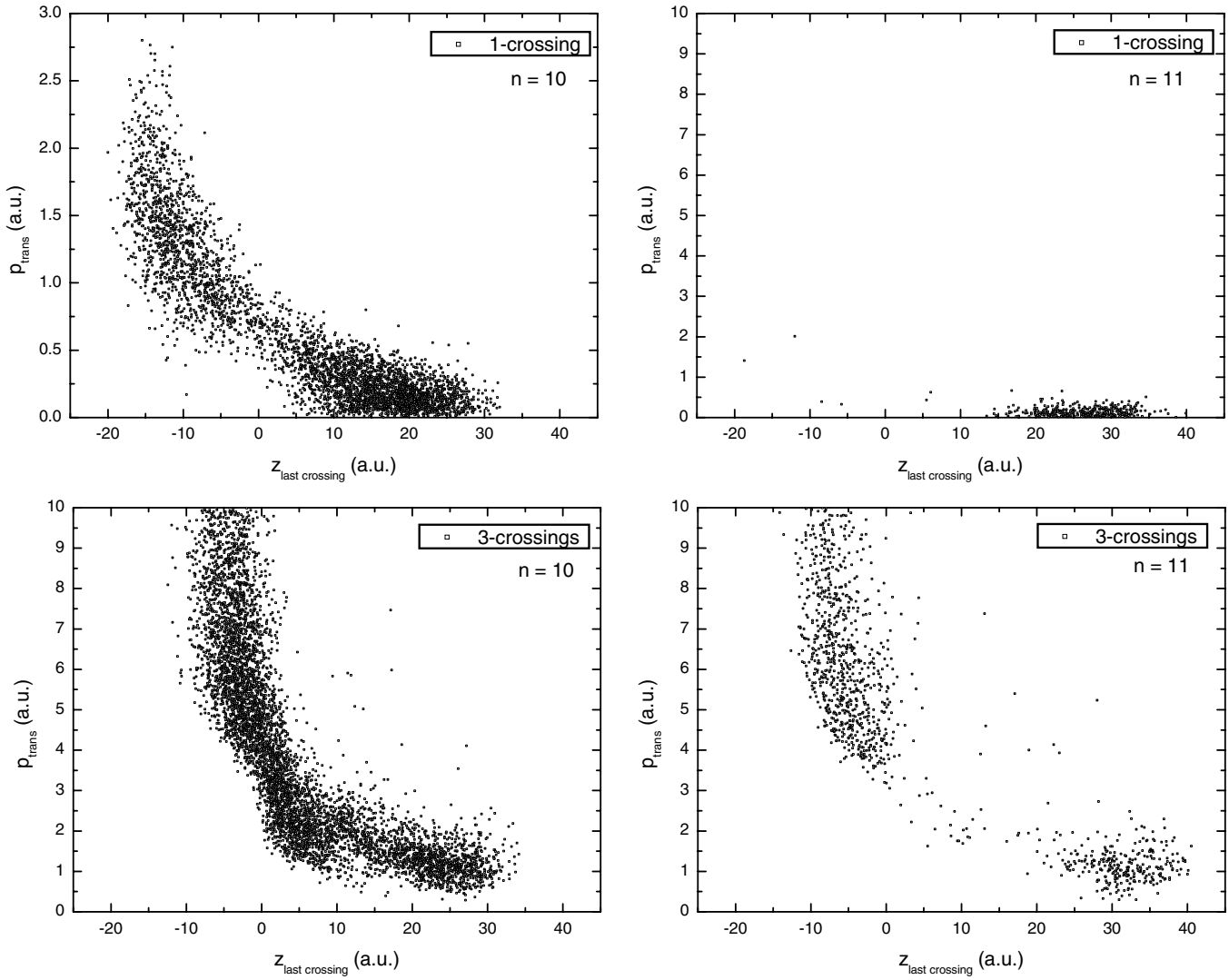

Figure 4. CTMC events plot of p_{trans} versus $z_{\text{last crossing}}$ for 1.5 keV/amu Ne^{8+}+Na(3s) collisions leading to electron capture to $n = 10$ and 11. The contributions from the 1- and 3-swap mechanism are explicitly shown.

structure with a maximum at about 5 au. These can be seen to be respectively related to collision events in the ranges (0 au $<$ $z_{\text{last crossing}} < +30$ au) and (-10 au $< z_{\text{last crossing}} < 0$ au). Moving to $n = 11$, we observe that the 1-swap mechanism leads to low p_{trans} values which can be associated with electronic capture by an already receding projectile ($+20$ au $< z_{\text{last crossing}} <$ $+35$ au). The 3-swap mechanism, on the other hand, clearly shows two peaks: one localized at about 1.1 au and the other at 4.8 au consisting in a much wider structure. These two structures are separated by an extended minimum at about 2–3 au. An inspection of the event plot displays that the peak at 1.1 au corresponds to electron capture by a receding projectile ($+25$ au $< z_{\text{last crossing}} < +40$ au), while the structure at 4.8 au corresponds to electron capture by an incoming projectile (-13 au $< z_{\text{last crossing}} < 0$ au).

We note that for the Na(3s) target the maximum impact parameter for which we collect single capture events within the CTMC method is approximately 35 au, independent of energy. We find this value in very good agreement with the COB value for the capture distance $R_C = (2\sqrt{Z_P} + 1)/|IP|$ which for the present collision system is 35.26 au. For increasing n-values, the projectile–target distances for the corresponding potential energy crossings are expected to increase as well. For $n = 9$ and 10, the energy crossings are found at 33.8 au and 53.03 au, respectively, indicating that capture to $n = 10$ is only possible via the excitation of the target in an early stage of the collision process. If we were to consider, for instance, an intermediate $Na^*(3p)$ state, we would find that the energy crossing distance for $n = 10$ is at 33.6 au which is within our impact parameter range. This implies that electron capture to n-values $\geqslant 10$ is only possible via the two-step process of the first target excitation followed by electron capture.

We note that for this system the swap oscillations are evenly spaced as a function of $1/v$, just as those in the total glory-scattering cross-section oscillations observed decades ago. However, in this case the interpretation is strictly classical in nature and not associated with quantal phases. The reason for the $1/v$ dependence is that the range of interaction is basically fixed at 35.0 au. Since the time of collision is roughly given by $T_C = 2b/v$, the collision time is simply a function of $1/v$ and

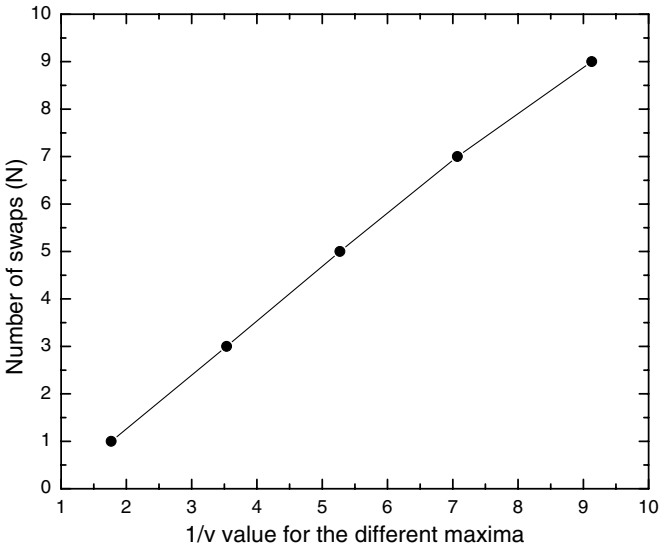

Figure 5. Number of swaps versus the $1/v$ values corresponding to the maxima of the corresponding N-swap-partial contributions to the $n = 10$ charge exchange cross section.

not also due to a changing range of interaction. For 2 keV/amu, the estimated collision time is 250 au, while the orbital time for an electron captured in the $n = 10$ level is approximately 100 au, indicating that 3-swaps are very likely as seen from the data. The swap oscillations become sharper for increasing n-values since the product Compton profiles decrease.

To illustrate the $1/v$ dependence of the swap oscillations we index the maxima of the 1-, 3-, 5-swaps by $N = 1$, 3, 5. The results for $n = 10$ are shown in figure 5. We note that the charge exchange oscillations observed for capture from Rydberg atoms are consistent with this interpretation [4]. Moreover, the oscillations observed on excitation total cross sections also follow this behaviour where now the maxima are indexed by even indices. Our differential data further display each individual swap signature at specific energies.

Conclusions

To summarize, in a joint experimental/theoretical exploration of low impact energy Ne^{8+} +Na(3s) collisions we have found direct evidence of an oscillatory structure in the angular p_{trans} distributions that is directly connected to the swap oscillations previously observed in the total cross sections for low charge-state ion collisions. The structure is very sensitive to the projectile impact energy. According to our CTMC results, the present structure is due to two reasons: (i) the number of swaps the electron can undergo across the potential saddle before it is captured and (ii) whether the electron capture (either for 1- or 3-swap) takes place in the incoming or outgoing parts of the projectile's trajectory. Electron capture by an incoming (outgoing) projectile leads to the structure at larger (lower) p_{trans} values. Since electron capture to n-values $\geqslant 10$ is only possible via the two-step process of the first target excitation followed by electron capture, the present theoretical results suggest that the excitation process can probably take place at different stages of the collision, providing in the incoming and outgoing channels feasible routes for capture, leaving as a result distinctive traces in the p_{trans} distribution.

The electron swap mechanism is present for capture to all n-levels and manifests itself in an oscillatory structure to capture high n-values where the swap oscillations have a lower frequency and sharper profile. Besides the present collision system, our preliminary data for other He-like ions like N^{5+} and O^{6+} [13] indicate that electron swaps are observed as well and are a natural extension of the widely used Coulomb-over-the-barrier model.

Acknowledgments

Work at KVI is sponsored by the Helmholtzzentrum für Schwerionenforschung GmbH (GSI), Germany–KVI University of Groningen collaboration agreement. Work at UNS supported by PGI 24/F049 of UNS and PIP 112-200801-02760 of CONICET (Argentina).

References

[1] Bernstein R B 1966 *Molecular Beams* ed J Ross (New York: Interscience) chapter 3 pp 75–134
[2] Perel J, Vernon R H and Daley H L 1965 *Phys. Rev.* **138** A937
[3] Olson R E 1969 *Phys. Rev.* **187** 153
[4] MacAdam K B, Day J C, Aguilar J C, Homan D M, MacKellar A D and Cavagnero N J 1995 *Phys. Rev. Lett.* **75** 1723
[5] Schultz D R, Reinhold C O and Krstic P S 1997 *Phys. Rev. Lett.* **78** 2720
[6] Krstic P S, Reinhold C O and Schultz D R 1998 *J. Phys. B: At. Mol. Opt. Phys.* **31** L155
[7] Niehaus A 1986 *J. Phys. B: At. Mol. Opt. Phys.* **19** 2925
[8] Flechard X, Nguygen H, Wells E, Ben-Itzhak I and DePaola B D 2001 *Phys. Rev. Lett.* **87** 123203
[9] Van derPoel M, Nielsen C V, Gearba M A and Andersen N 2001 *Phys. Rev. Lett.* **87** 123201
[10] Turkstra J M, Hoekstra R, Knoop S, Meyer D, Morgenstern R and Olson R E 2001 *Phys. Rev. Lett.* **87** 123202
[11] Knoop S, Olson R E, Ott H, Hasan V G, Morgenstern R and Hoekstra R 2005 *J. Phys. B: At. Mol. Opt. Phys.* **38** 1987
[12] Blank I, Otranto S, Meinema C, Olson R E and Hoekstra R 2012 *Phys. Rev.* A **85** 022712
[13] Blank I, Otranto S, Meinema C, Olson R E and Hoekstra R 2012 in preparation
[14] Garvey R H, Jackman C H and Green A E S 1975 *Phys. Rev.* A **12** 1144
[15] Becker R L and McKellar A D 1984 *J. Phys. B: At. Mol. Phys.* **17** 3923